JMEPEG (2001) 10:515–520

Microstructural Modification in a Laser-Treated 2.25Cr-1Mo Steel

R.V. Subba Rao, P. Parameswaran, and R.K. Dayal

(Submitted 11 April 2000; in revised form 30 March 2001)

A systematic study was carried out to understand the various microstructural changes in the heat-affected zone due to laser treatment on 2.25Cr-1Mo steel. The observed microstructures pertain to different cooling rates at different depths from the surface. A good correlation of the microstructures with the corresponding time-temperature-transformation (TTT) diagram of the steel was observed.

Keywords 2.25Cr-1Mo steel, laser surface treatment, microstructures

1. Introduction

Lasers are currently employed in high-speed precision jobs such as cutting and joining in most industries. Further, being a controlled heat source, laser finds potential application for transformation hardening of components made of carbon steels.[1,2] The rapid heating rates and the associated cooling rates make this process capable of providing a wide range of microstructures with different mechanical properties within a very shallow depth of the surface. Thus, it could be quite useful in the fabrication of thin-walled heat exchangers, where tungsten inert gas (TIG) welding is presently employed.[3] The present problems due to TIG welding, namely, stress arising from rigid fastening, distortion, and vibrations could be avoided if an alternative method such as laser welding is attempted. The major advantages of the laser process are as follows:

- minimal or no damage/distortion of the workpiece; and
- rapidity of the single shot laser process.

Whenever a laserlike source is used to join a thin sheet material to thick-walled ones, it is necessary that the weldment should have adequate mechanical properties. In other words, microstructural similarity to the parent material must be generated during the weld thermal cycle. The heat flow problems in the laser process are quite complicated by the number of variables involved. They can be either process parameters such as beam size, power, absorbtivity, or material parameters such as specific heat and thermal conductivity.

Considering the fact that laser processing offers a comprehensive solution, a systematic study by varying the power of the laser source to determine the nature of microstructure that evolves in a ferritic low alloy 2.25Cr-1Mo steel is carried out. The melting of thin layers of metal surfaces by directed laser beam would result in rapid resolidification. Consequently, the surface and subsurface microstructures are modified. Several distinct microstructural zones are expected to develop from the laser-melted surface end to depths of a few hundred microns due to the heat input imposed by the laser source at the surface and the differential cooling rates envisaged by successive zones. The present paper reports the modification of the microstructure as a consequence of irradiation with a low power laser source.

R.V. Subba Rao, P. Parameswaran, and **R.K. Dayal,** Materials Characterization Group, Indira Gandhi Centre for Atomic Research, Kalpakam 603 102 India. Contact e-mail: rkd@igcar.ernet.in.

2. Experimental

The nominal composition of the low alloy ferritic steel used in this study is shown in Table 1. The material was supplied in the form of plates from which specimens of $5 \times 7 \times 10$ mm were cut and degreased using alcohol. Samples were heat treated in two different conditions: normalized (hereafter referred as N) condition (1323 K for 1 h) and normalized and tempered (hereafter referred as N&T) condition (1323 K/1 h followed by 1023 K for 0.5 h). In all cases, following the heat treatment, the samples were cooled in still air. The heat-treated samples were polished and degreased prior to laser treatment.

An indigenous, multibeam, continuous wave CO_2 laser system operating at 10.6 μm was used for the laser treatment. This system has a slow axial flow type of construction and uses a ZnSe lens to focus the six beams onto the specimen. It could deliver a maximum power of 500 W. In the present study, autogenous laser spots at three different power levels, 100, 150, 200 W, were produced. The laser beam was focused onto the surface of the plate and had a circular shape with Gaussian distribution of energy. The beam diameter was estimated to be 1.5 mm. The power densities were of the order of 10^8 W/m^2. The time of exposure was maintained at 30 s in all the treatments.

The irradiated samples were cut across the spot and the cross sections were examined in an optical microscope, MeF4A (M/sLeica, Vienna, Austria), and scanning electron microscope (PSEM 501, Philips Electron Optics, Eindhoven, The Netherlands). Microhardness profiles of the same samples were determined using a load of 50 and 10 g using a Vickers microhardness tester.

3. Results and Discussion

3.1 Initial Microstructures of the Steel

The heat treatment at N condition resulted in a fully bainitic microstructure, as shown in Fig. 1(a). The samples heat treated

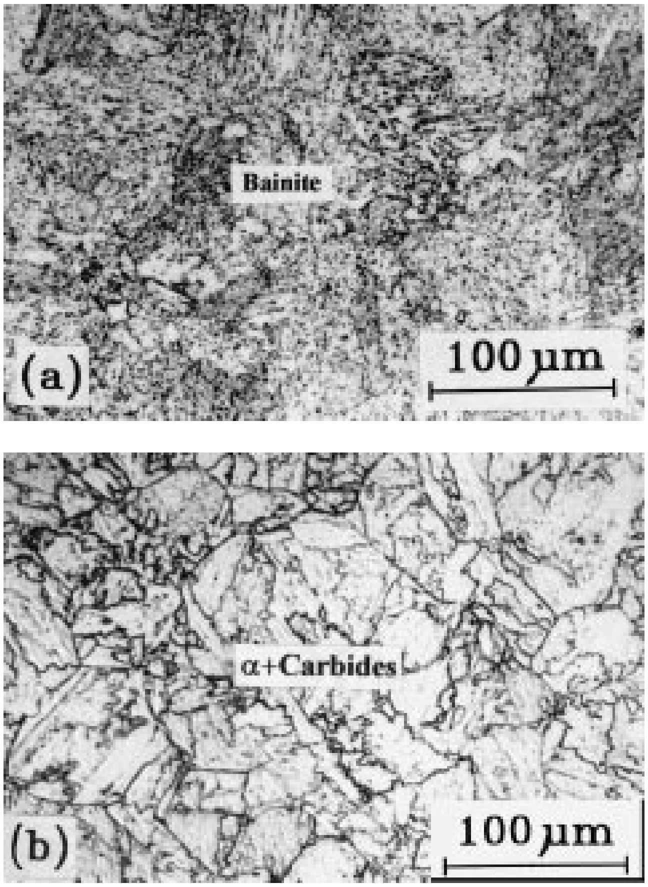

Fig. 1 Optical micrograph showing the initial microstructure: (**a**) fully B in N condition and (**b**) tempered B (α + carbides) in N&T condition

Table 1 Chemical composition of the steel used

Elements	Cr	Mo	C	Si	Mn	P	Fe
Wt.%	2.21	0.9	0.11	0.31	0.4	0.025	Rest

Table 2 Width of different zones

	Width of zones (in μm)	
Laser power (in W)	**Melt zone**	**Heat-affected zone**
100	180	3300
150	200	4780
200	260	5210

under N&T condition exhibited a tempered microstructure, namely, ferrite (α) and carbides, as given in Fig. 1(b).

3.2 Microstructure after Laser Surface Treatment

Laser surface treatment melted the surface layers. The depth of surface-melted zones varied from 100 to 200 μm for the range of power employed, *viz.* 100 to 200 W. From the optical micrographs, the widths of different zones were measured and the values are furnished in Table 2.

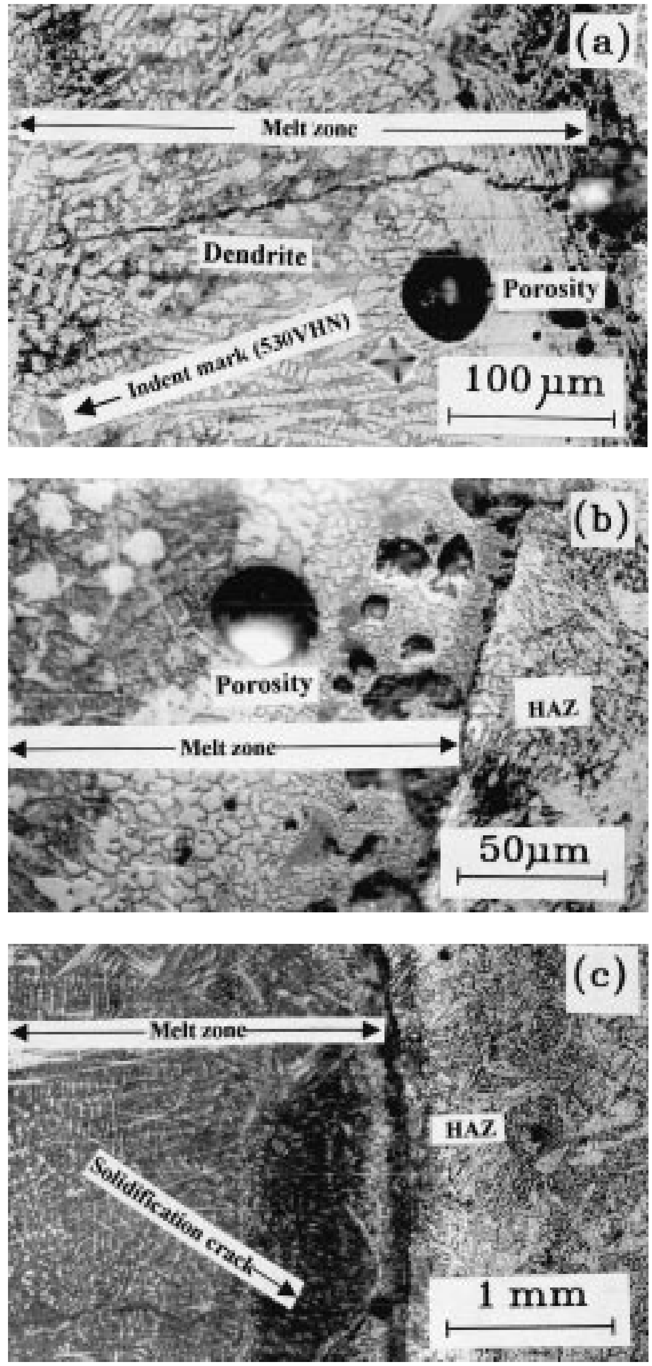

Fig. 2 Optical micrograph showing the widths of melt zones for three different laser powers: (**a**) 100 W, (**b**) 150 W, and (**c**) 200 W

The Melt Zone. The solidified zones close to the surface exhibited a dendritic microstructure due to the high rate of cooling experienced by the surface. The zones further had developed cracks and porosity probably because of tensile residual stresses present locally. Figure 2 compares the microstructures at the surface for the three power inputs. Although the microstructures are similar in their nature, the width of the dendritic area of the sample irradiated with 200 W was about 2 times that of the sample irradiated with 100 W (Fig. 2a and c). The

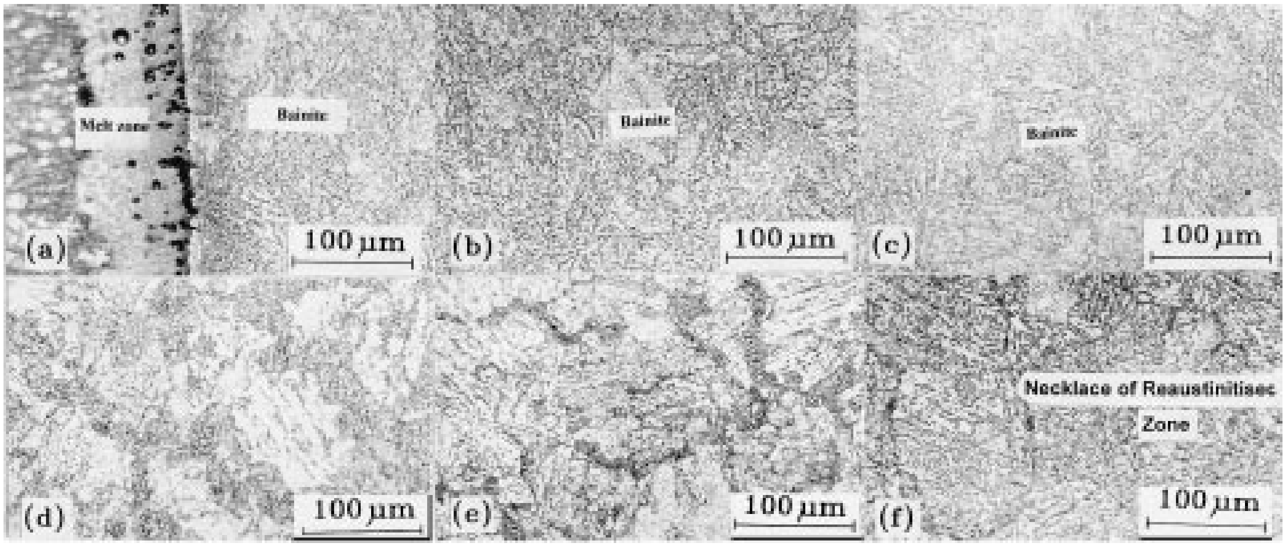

Fig. 3 (**a**) to (**f**) A series of optical micrographs showing the microstructural modification due to laser treatment (150 W/30 s) in samples of N condition

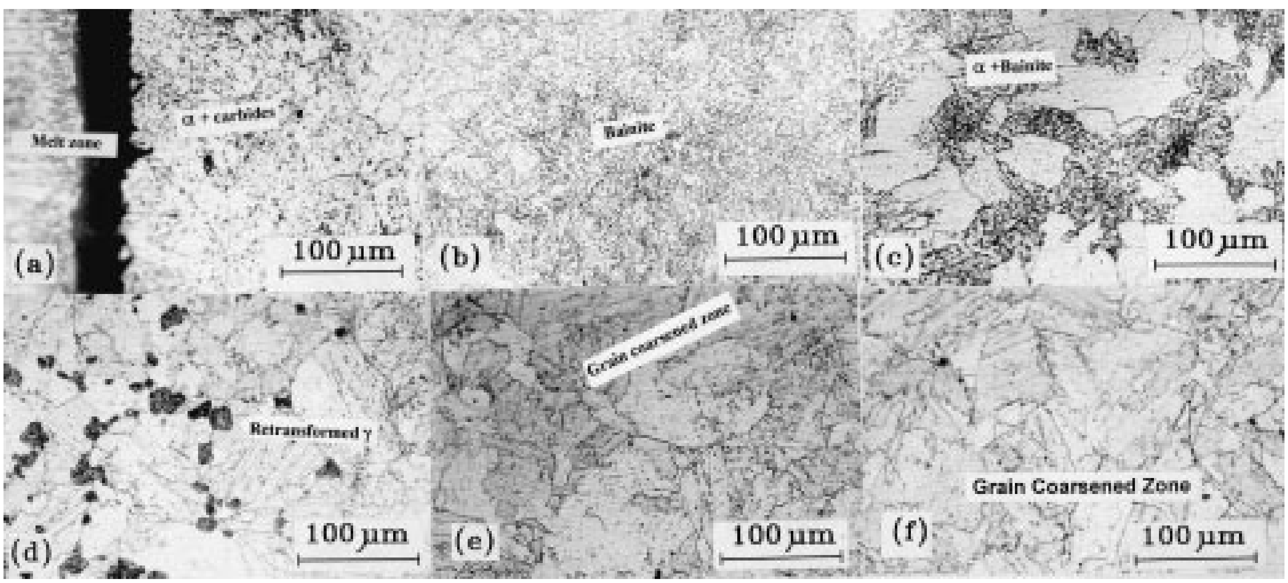

Fig. 4 (**a**) to (**f**) A series of optical micrographs showing the microstructural modification due to laser treatment (150 W/30 s) in samples of N&T condition

microhardness of these regions was measured and found to be 530 VHN, indicating that the zone is hard.

Distinct Heat-Affected Zones. Beneath the melt layer, only solid-state transformation occurred and the products of austenite resulting from a range of cooling rates were observed. These products of austenite for two different initial microstructural conditions are discussed in the following section.

N Condition. Figures 3(a) to (f) show the microstructures corresponding to the adjacent layers of laser-modified surface of the N sample treated with 150 W. A typical bainitic structure was observed, as shown in Fig. 3(a) to (c), while Fig. (d) and (e) exhibited a mixed structure of partially reaustenitized necklaces with tempered α regions. The microstructure present in Fig. 3(f) exhibited again a fine necklace of reaustenitized zone, but the bainitic structure was retained with coarser prior austenite grains.

Similar structures were obtained for other power inputs (100 and 200 W) of laser irradiation.

N&T Condition. The micrographs shown in Fig. 4 (a) to (f) correspond to the different products that evolved from the laser treatment of a N&T sample. The layers beneath the melted zone exhibited fine α grains with profuse carbide precipitation. (Fig. 4a). This is in contrast to what was observed in a N sample. In zones farther away, a microstructure somewhat bainitic in morphology appeared, with fine prior austenite grains. It can be inferred that the structure is partially tempered. Figure 4(c)

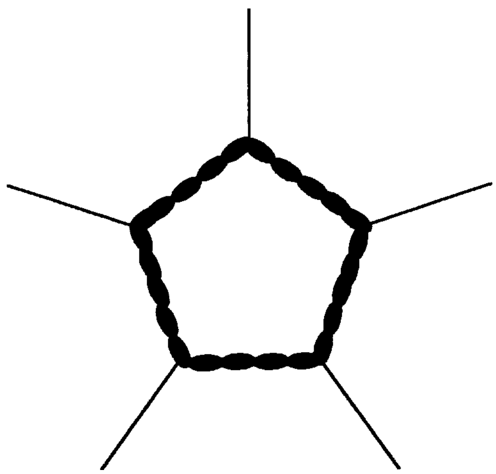

(a)

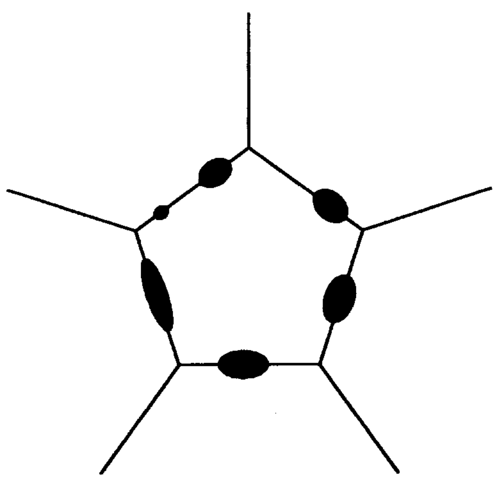

(b)

Fig. 5 (**a**) Schematic figure depicting the nucleation of austenite along the grain boundary generating a necklacelike structure in the N sample. (**b**) Schematic figure depicting the discrete nucleation of austenite around the carbides in the N&T sample

and (d) show the microstructures of regions that have experienced the temperature of the two-phase regime, namely, $\{\alpha +$ austenite$\}$ of the Fe-C phase diagram. The resulting structure consists of a matrix of α with islands of partially transformed austenite products. A similar observation was reported by Duke *et al.*[4] for the case of 12Cr-1Mo steel. In the present steel, the transformed austenite products could be α with carbides such as M_2C, M_7C_3, and $M_{23}C_6$. The systematic evolution of the various carbides has been discussed elsewhere.[5,6]

In comparison, the N sample exhibited a fine necklace of partially austenite zone, while it was not present in the N&T sample. This can be explained based on the fact that the carbides already present in the initial microstructure in the case of the N&T sample acted as centers of nucleation for austenite to grow, while in the other case, the grain boundary acted as the nucleation site. This is schematically shown in Fig. 5(a) and (b).

The microhardness profiles of the samples indicate a significant drop in hardness around 100 to 200 μm distance from the

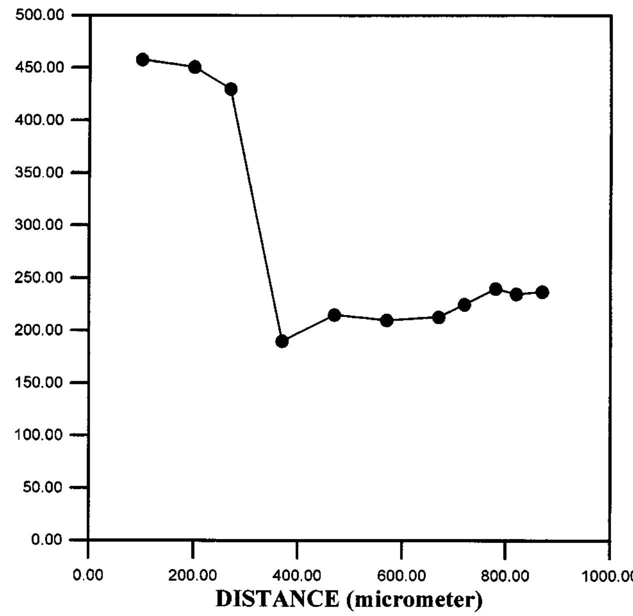

(a)

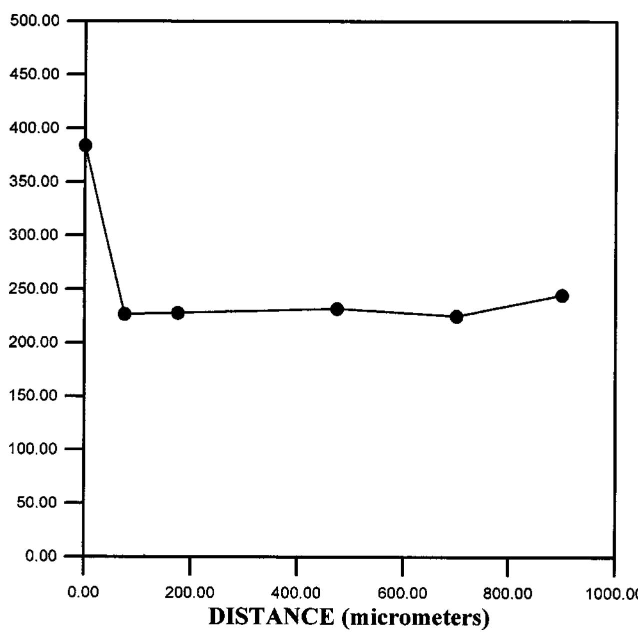

(b)

Fig. 6 Hardness profiles of samples treated with a laser beam of power 150 W for 30 s in (**a**) N condition and (**b**) N&T condition

laser-surface-melted end for the cases of both N and N&T conditions (Fig. 6a and b).

The generation of the above-discussed distinct microstructures is due to the differential cooling rates seen by the different sections as the heat is passed over from the melt end to the interior. In order to understand the heat distribution, the following simplified calculations were carried out.

When the surface of the steel samples was struck with a beam of laser at 100 to 200 W power, the laser spots melted the surface. The transmitted energy that reaches a depth of *z*,

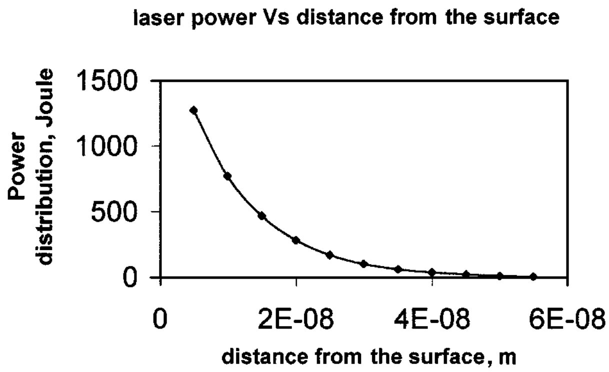

(a)

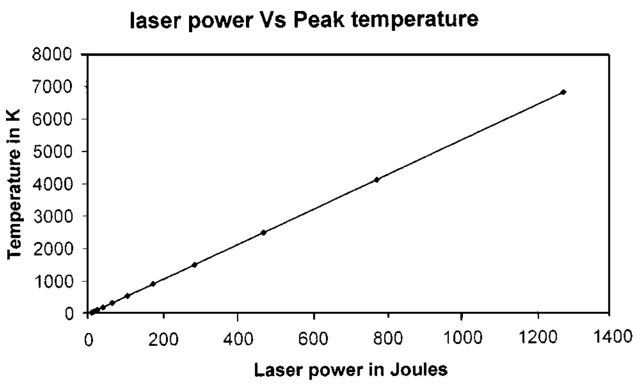

(b)

Fig. 7 (**a**) Typical estimate of distribution of power along the cross section of the samples. (**b**) Corresponding peak temperatures generated along the cross section of the samples

due to laser irradiation, can be calculated using the Lambert-Beer law:[7]

$$E(z,t) = Eo(t)(1 - R)\exp(-\alpha z) \qquad \text{(Eq 1)}$$

where $E(z,t)$ is the energy transmitted to a depth of z, and t is the time of exposure while $Eo(t)$ is the total energy for t s, $(1 - R)$ is a factor of absorbtivity, R is the reflectivity, α is the absorption coefficient, and z is the depth.

The above equation can be used to generate the power distribution in the sample as a function of distance from the irradiated end (Fig. 7a). It can be inferred from the figure that the power distribution that resulted from the laser irradiation time of 30 s is found to drop down within 20 to 40 nm layers. However, the heat was transmitted toward inner layers beneath according to the Fourier law of heat conduction.

The peak temperature obtained at the surface can be calculated[8] incorporating the various experimental parameters as follows:

$$T_{\text{gaussian}} - T_{\text{amb}} = 2P/(\pi^2 aK) \qquad \text{(Eq 2)}$$

where P is the total power absorbed on the surface, α is the diameter of the beam, and K is the thermal conductivity of the steel. The relationship is shown in Fig. 7(b). The combination of the powers and the interaction time was chosen in such a way

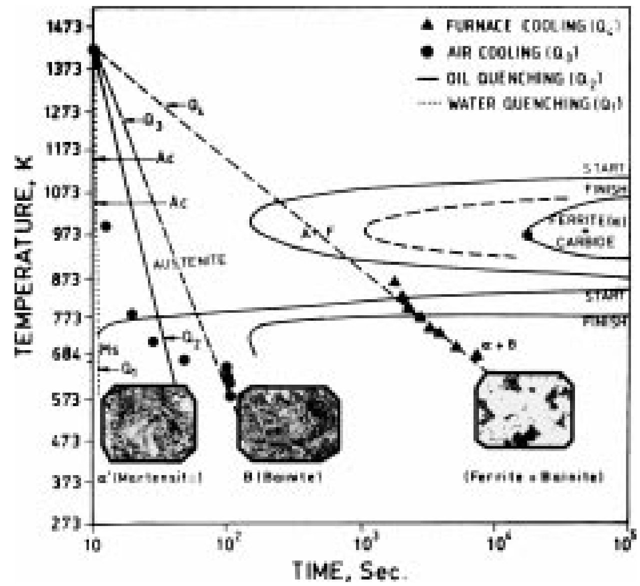

Fig. 8 A map of the TTT diagram of the 2.25Cr-1Mo steel[8] superimposed with the microstructures obtained by laser treatment

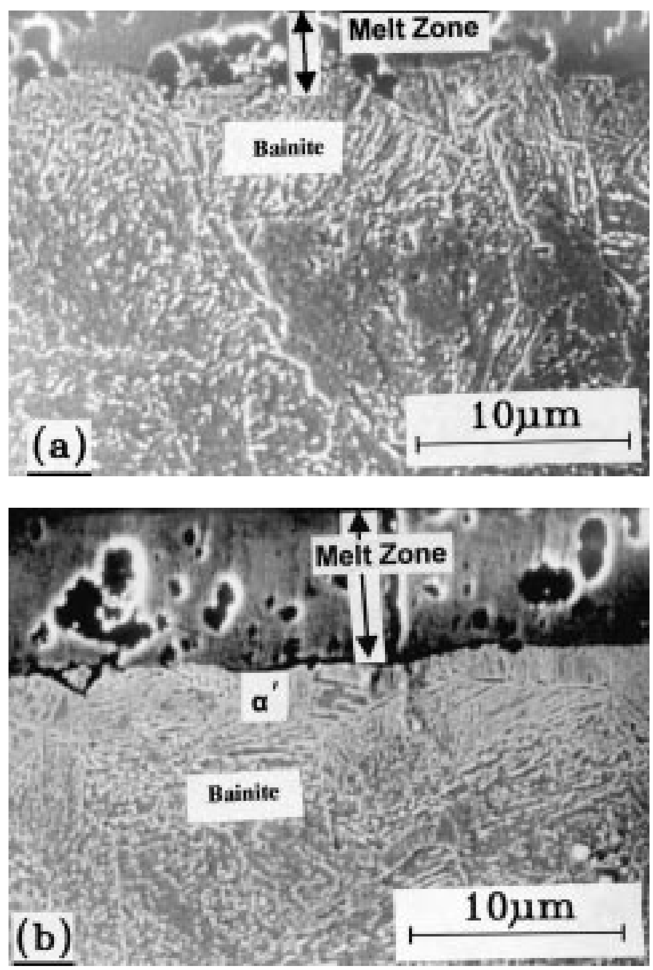

Fig. 9 Secondary electron micrograph of (**a**) N sample treated with 100 W and (**b**) N sample treated with 150 W

that the surface layers melted in all the cases. The consequent microstructural modification with reference to different cooling rates experienced is discussed below:

The laser irradiation brought about a series of microstructures that correspond to either one or a combination of phases such as martensite (α'), bainite (B), and bainite (B) + ferrite (α). The hardness values of the individual phases α and B were found to be 144 and 259 VHN, respectively. Further, in order to understand the nature of the evolution of these microstructures, the time-temperature-transformation (TTT) diagram[9] of the 2.25Cr-1Mo steel, along with four different cooling rates, namely, water quenching (Q1), oil quenching (Q2), air cooling (Q3), and furnace cooling (Q4), imposed over it, is presented in Fig. 8. The microstructures that result from these cooling rates were found to be α', B, B and (B + α) respectively. Typical microstructures obtained from this work were presented in the map along with the TTT diagram. It can be inferred that a steep cooling rate equaling that of water quenching can result in α', while a slower cooling rate similar to furnace cooling can result in α + B.

Figure 9(a) shows that, for the case of 100 W irradiation, there is no α' along the liquid solid interface, while Fig. 9(b) shows clearly the formation of a fine α' zone of width ~5 μm in a sample treated at 150 W. This can be attributed to a higher power density, which causes the steel to experience a steep rate of heating as well as cooling.[10] Hence, it appears that there exists a minimum power density to favor the formation of α'. In the sample irradiated with 200 W power, the α' is again present.

It can be concluded from the above results that the various types of microstructure could be achieved by effective control of the power input during laser melting.

4. Summary

- Systematic microstructural characterization of various zones present in a laser-surface-treated 2.25Cr-1Mo steel was carried out.
- The hardness of different zones exhibited a good correspondence with the microstructures observed.
- A map portraying the various phase field zones, the corresponding TTT diagram of the steel, and the microstructures was presented to show the effectiveness of surface modification by laser surface treatment in achieving a variety of microstructures.

Acknowledgments

The authors acknowledge Dr. V.S. Raghunathan, Associate Director, Materials Characterization Group, and Dr. H.S. Khatak, Head, Corrosion Science and Technology Division, for their keen interest and constant encouragement during the course of the work. The authors also acknowledge Ms. M. Vijayalakshmi and Dr. P. Muraleedharan for the fruitful discussions and Mr. V. Thomas Paul for his help during the experimental stages.

References

1. R.K. Shiue and C. Chen: *Metall. Trans. A,* 1992, vol. 23A , pp. 163-70.
2. Andrew Kopel and Wayne Reitz: *Adv. Mater. Proc.,* 1999, vol. 9, pp. 39-41.
3. Hrivnak Ivan: *Theory of Weldability of Metals and Alloys,* Elsevier, Amsterdam, The Netherlands, 1992, p. 235.
4. Richard K. Duke, Po-shou Chen, and R.C. Wilcox: *Metallography,* 1988, vol. 21, pp. 347-58.
5. R.G. Baker and J. Nutting: *J. Iron Steel Inst.,* 1959, vol. 192, pp. 257-308.
6. S. Saroja, P. Parameswaran, M. Vijayalakshmi, and V.S. Raghunathan: *Acta Metall. Mater.,* 1995, vol. 43, pp. 2985-3000.
7. A. Frenk, A.F.A. Hoadley, and J.D. Wagniere: *Metall. Trans. B,* 1991, vol. 22B, pp. 139-41.
8. R.C. Crafer and P.J. Oakley: *Laser Processing in Manufacturing,* Chapman and Hall, London, 1993, p. 36.
9. P. Parameswaran, S. Saroja, M. Vijayalakshmi, and V.S. Raghunathan: *JNM,* 1996, vol. 232, pp. 226-32.
10. Tadeusz Burakowski and Tadeusz Wierzchon: *Surface Engineering of Metals,* CRC Press, New York, NY, 1998, p. 340.